

Macroseggregation and Nucleation in Undercooled Pb-Sn Alloys

Henry C. de Groh III
Lewis Research Center
Cleveland, Ohio

(NASA-TM-102023) MACROSEGREGATION AND
NUCLEATION IN UNDERCOOLED Pb-Sn ALLOYS
(NASA, Lewis Research Center) 36 pCSCL 11F

N89-23664

Unclas
G3/26 0210770

May 1989

NASA



CONTENTS

	Page
ACKNOWLEDGMENTS	11
SUMMARY	1
INTRODUCTION	1
EXPERIMENTAL PROCEDURE	4
Apparatus	5
Undercooling and Solidification Procedure	6
RESULTS	7
DISCUSSION	10
Nucleation	10
Macrosegregation	11
CONCLUDING SUMMARY	12
APPENDIX A	14
APPENDIX B	15
REFERENCES	16
TABLES	17
FIGURES	19



ACKNOWLEDGMENTS

The author wishes to thank the staff of the Microgravity Materials Science Laboratory and others for their contributions and assistance to this project: Richard Rauser for help with metallography, David Lee for help with the experimental work and data collection, Steve White and Bruce Rosenthal for assistance with hardware, Judy Auping for guiding me through the computer software, and Francis Terepka and David Hull for doing the extensive microscopy and microprobe analysis. Special thanks and recognition are due Dr. V. Laxmanan and Dr. John F. Wallace for their time and technical guidance.



MACROSEGREGATION AND NUCLEATION IN UNDERCOOLED Pb-Sn ALLOYS

Henry C. de Groh III
National Aeronautics and Space Administration
Lewis Research Center
Cleveland, Ohio 44135

SUMMARY

A novel technique resulting in large undercoolings in bulk samples (23 g) of lead-tin alloys was developed. Samples of Pb-12.5 wt % Sn, Pb-61.9 wt % Sn, and Pb-77 wt % Sn were processed with undercoolings ranging from 4 to 34 K and with cooling rates varying between 0.04 and 4 K/sec. The nucleation behavior of the Pb-Sn system was found to be nonreciprocal. The solid Sn phase effectively nucleated the Pb phase of the eutectic; however, large undercoolings developed in Sn-rich eutectic liquid in the presence of the solid Pb phase. This phenomenon is believed to be mainly the result of differences in interfacial energies between solid Sn-eutectic liquid and solid Pb-eutectic liquid rather than lattice misfit between Pb and Sn. Large amounts of segregation developed in the highly undercooled eutectic ingots. This macrosegregation was found to increase as undercooling increases. Macrosegregation in these undercooled eutectic alloys was found to be primarily due to a sink/float mechanism and the nucleation behavior of the alloy. Lead-rich dendrites are the primary phase in the undercooled eutectic system. These dendrites grow rapidly into the undercooled bath and soon break apart due to recalescence and Sn enrichment of the liquid. These fragmented Pb dendrites are then free to settle to the bottom portion of the ingot causing the macrosegregation observed in this study. A eutectic Pb-Sn alloy undercooled 20 K and cooled at 4 K/sec had a composition of about Pb-72 wt % Sn at the top and 55% Sn at the bottom.

INTRODUCTION

The macro and microstructures of metals and alloys are strongly influenced by the undercooling achieved prior to solidification, the nucleation characteristics of the alloy, and the cooling rate imposed during solidification (refs. 1 and 2). In general, the amounts of macro and microsegregation in metal castings decrease with increases in undercooling, nucleation, and cooling rate. At higher undercoolings and faster cooling rates, local solidification times are decreased, thus a more homogeneous product is expected. Macro and microsegregation are generally detrimental to the engineering properties of the alloy, therefore increases in undercooling and cooling rate are usually desired. Under some circumstances, however, increases in undercooling and cooling rate can increase macro and microsegregation. Microsegregation in an undercooled alloy may be augmented by the preferential nucleation of a particular phase and the growth of this phase driven by undercooling. Macrosegregation requires significant movement of solute rich or solute poor solid or liquid within the ingot. This movement is usually driven by a sink/float mechanism. The density differences which cause gravity driven macrosegregation are typically caused by differences in liquid and solid compositions. Gravity driven macrosegregation is common in the casting of cast irons and in other eutectic systems and may be compounded by thermal cycling near the eutectic temperature (ref. 3). The density difference between the liquid and solid phases and the ability of the

E-4759

Pb-Sn eutectic to be undercooled are favorable for the study of macrosegregation and the influence of undercooling on segregation behavior. The objectives of this work were (1) to study how macrosegregation is affected by the initial undercooling of the melt and (2) to devise means to control macrosegregation.

In order to undercool liquid metal, heterogeneous nucleation must be limited. To decrease heterogeneous nucleation, potentially active sites must be either removed from the liquid or deactivated. A potentially active site must be both a solid and in contact with the liquid. Undercooling may be achieved by dispersion of a liquid sample into a very large number of fine, independent droplets. In this case, if the number of droplets is much greater than the number of active nucleation sites, a large fraction of the droplets will have "no" nucleation sites and thus will undercool. Larger samples are usually covered on all sides with a glassy (noncrystalline) slag or flux which in effect removes the liquid alloy from the solid crucible. The slag also dissolves and collects impurities from the bath, cleaning it and helping it to undercool.

The nucleation behavior of Pb-Sn, and many other alloys, has been studied using fine droplets ($\approx 20 \mu\text{m}$ in diameter weighing $\approx 4 \times 10^{-8}$ g) (refs. 4 to 7). In these studies the nucleation behavior of Pb-Sn was shown to be nonreciprocal; i.e., the Pb-rich phase is a poor nucleant for the Sn-rich phase, while the Sn-rich phase appears to be an effective nucleant for the Pb-rich phase. Many other alloys such as Pb-Au, Bi-Au, Bi-Ag, and Tl-Sn have been shown to have nonreciprocal nucleation behavior. This nucleation behavior is explained by solid-liquid interfacial energy barriers to nucleation, rather than by lattice misfit between the nucleating catalyst and potential solid (refs. 5 and 8). The interfacial energy balance of Pb and Sn heterogeneously nucleating on an essentially flat surface of Sn and Pb respectively is shown in figure 1. As in figure 1, when Pb is nucleating on Sn the balance of interfacial energies is given by,

$$\gamma_{\text{Sn}} = \gamma_{\text{PbSn}} + \gamma_{\text{Pb}} \cos \phi$$

and when Sn is nucleating on Pb,

$$\gamma_{\text{Pb}} = \gamma_{\text{PbSn}} + \gamma_{\text{Sn}} \cos \theta$$

where the interfacial energy of Pb in contact with eutectic liquid is γ_{Pb} , Sn-eutectic liquid is γ_{Sn} , and the energy associated with the solid Pb-Sn interface is γ_{PbSn} . The relative wetting angles of the nucleating spherical caps are determined by the solid-liquid surface energies such that,

$$\frac{\gamma_{\text{Pb}}}{\gamma_{\text{Sn}}} = \frac{(1 + \cos \theta)}{(1 + \cos \phi)}$$

Gündüz and Hunt experimentally determined solid-liquid surface energies for the Pb-Sn eutectic alloy (ref. 9). They found the solid-liquid interfacial free energies of saturated solid Pb and Sn in contact with eutectic liquid to be 56 and 132 erg/cm² respectively. Assuming a value of 10° for the wetting angle of Pb on Sn, ϕ , the angle for the Sn cap, θ , is 100°.

In order to form a stable, heterogeneously nucleated cap of solid, the nucleation barrier ΔG_n must be surpassed. The probability of achieving this energy is proportional to $\exp(-\Delta G_n/kT)$ (ref. 10); thus, the probability of nucleating Pb on Sn relative to nucleating Sn on Pb in the Pb-Sn eutectic alloy is given by

$$P = \frac{\exp(-\Delta G_{Pb}/kT)}{\exp(\Delta G_{Sn}/kT)}$$

where ΔG_{Pb} is the nucleation energy barrier to Pb nucleating on Sn, and ΔG_{Sn} is that of Sn nucleating on Pb. Following classical nucleation theory it can be shown that for a spherical cap of effective radius equal to the critical radius required for stability, the nucleation activation energy is (ref. 10)

$$\Delta G_n = \frac{16\pi\gamma^3 f}{3(\Delta S_f \Delta T)^2}$$

where:

γ = interfacial energy between the nucleating cap and the liquid

$f = (2 + \cos \delta)(1 - \cos \delta)^2/4$, where δ is the contact angle of the cap

$\Delta S_f = \Delta H_f/T_m$, the entropy of fusion, assumed constant for Pb and Sn

ΔT = undercooling, $T_m - T$

As shown in appendix A the probability ratio, P , of nucleating Pb on Sn rather than Sn on Pb in the eutectic is nearly infinite ($>10^{500}$), indicating that Pb should nucleate on Sn at a negligible undercooling compared to the undercooling required for nucleation of Sn on Pb. Thus, in the absence of other heterogeneous substrates, theory predicts that in a hypoeutectic Pb-rich alloy, the enriched liquid remaining after growth of Pb dendrites will undercool below the equilibrium eutectic temperature to a greater extent than the enriched eutectic liquid of a hypereutectic alloy. This phenomena has been shown to occur in experiments, showing good agreement with theory (refs. 4, 5, 7, 13, and 14).

Also shown in appendix A is the probability ratio of homogeneously nucleating Pb relative to Sn in the undercooled Pb-Sn eutectic. As is found in experiments, Pb is predicted to be the primary phase in the eutectic alloy (ref. 7). In the eutectic alloy, the heavier Pb-rich dendrites which grow first may settle to the ingot bottom (ref. 14); however, such sedimentation processes, and other macrosegregation phenomena, cannot be studied using fine droplets. Undercooled, larger sized samples are needed to study these effects.

Most of the bulk undercooling literature has centered around studies of dilute alloys (ref. 15), dendrite velocity measurements (ref. 16), and alloys with small differences in density between components (refs. 17 and 18). Davis et al. studied grain structure and solute distribution in undercooled pure Bi

and Bi-100 ppm Ag alloys (ref. 15). They reported no significant macrosegregation; and none should have been expected due to the small difference in composition between the solid and liquid phases. The structure and mechanical properties of undercooled Ni-30% Cu, Ni-20% Cr, and Fe-25% Ni alloys were analyzed in a study by Kattamis and Mehrabian; these authors found the structure and composition of the undercooled alloys to be highly uniform and homogeneous (ref. 17). Macrosegregation is again not expected due to the small variations in densities between phases. Tewari has studied the undercooling behavior and structures of Mo-Ni eutectic and hypoeutectic alloys (ref. 19). Tewari observed large amounts of microsegregation; however, since his samples were only about 3 mm diameter with no definite orientation relative to gravity, no macrosegregation was observed.

The lead-tin system has much larger density differences between phases than the alloys mentioned above. Assuming ideal solutions and 3 vol % shrinkage during solidification, the density ratio of the solid Pb-rich phase of the eutectic (Pb-19.2% Sn) and the eutectic liquid (Pb-61.9% Sn) is about 1.2 (appendix B). Johnson and Griner observed macrosegregation in a study of Pb-Sn eutectic alloys in which the gravitation field was varied through use of a centrifuge (ref. 20).

The objective of this research was to determine how macrosegregation is affected by initial undercooling and cooling rate prior to nucleation. Bulk sized samples (≈ 23 g) of Pb-Sn were solidified with initial undercoolings of between 4 and 34 K and cooling rates ranging from 0.04 to 4 K/sec. The compositions studied were Pb-12.5 wt % Sn, Pb-61.9 wt % Sn, and Pb-77 wt % Sn. These compositions were used because they: (1) enabled the study of primary phase undercooling as well as secondary phase undercooling in the presence of the primary phase, and (2) had been previously studied by others using droplets, thus enabling the comparison of the two processes and the possible extension of the previous work to large ingots and the observation of the impact of undercooling on bulk samples. Post-solidification metallography of the overall structures was used to help determine whether gravity driven convection in the liquid state or gravitational settling of dendrite fragments was the primary mechanism leading to macrosegregation. Microprobe analyses of composition variations was conducted to quantitatively determine varying macrosegregation levels among undercooled ingots.

EXPERIMENTAL PROCEDURE

Ingots of Pb-12.5 wt % Sn, Pb-61.9 wt % Sn, and Pb-77 wt % Sn were prepared from 99.999 percent pure Pb and Sn shot. The volume and geometry of all the ingots were 2.7 cm^3 , contained vertically in glass tubes with an inside diameter measuring 0.5 in. Figures 2 and 3 show the phase diagram with the compositions studied and a schematic of the ingot, crucible, and thermocouple locations. All ingots were about 1 in. tall and solidified with two thermocouples immersed in the bath. The thermocouples were either Pyrex or fused silica sleeved, Type K, and located about 5 mm down from the top and 5 mm up from the bottom. The accuracy of the thermocouples was periodically checked using pure Sn and found to be within 0.5 K at 231.9 °C. Ingots were covered with Dow Corning 704 diffusion pump oil to prevent wetting of the glass crucible and promote easy removal of the solidified sample.

Apparatus

Two different apparatus were used to process the ingots: the bulk undercooling furnace (BUF hereafter) (fig. 4), and a vertical tube furnace contained inside a glove box. Both furnaces had certain desired advantages. The BUF is a three-zone resistance heated stainless steel tube furnace. The sample heating and cooling rates, soak time, and thermal gradient can be more closely controlled in the BUF than in the glove box. The heater bands of the BUF are 1 in. in length, thus only the bottom two were needed to produce the desired heating profile. A Hewlett Packard computer (HP-85B) is used to control the power supplies and cooling fluid of the BUF and facilitate the measurement and recording of the thermal history of experiments. Experiments are setup and programmed into the computer so that they may be run by the computer. Temperatures recorded by various thermocouples (a maximum of six) are monitored through a HP 3497 Data Logger interface. The software incorporated in the HP-85B implements a proportional-integral-differential control algorithm for the power supplies and also samples the thermocouple outputs at data scan rates up to 1 Hz. Ingots are sealed in the BUF and an argon purge maintained during the experiments. Thermocouples are inserted through tight fitting holes in a Teflon insert at the top of the furnace.

Samples processed in the BUF were put through the controlled heating, soak, and cooling procedure shown in figure 5. The soak temperature was 350 °C for the Pb-12.5 wt % Sn alloy because of its higher liquidus. The power to the heater bands was turned off at the end of the soak and the bottom of the furnace quenched with water during the cooling and solidification cycle of each experiment. The cooling rates were approximately 0.7 °C/sec and the thermal gradients were about 6 °C/cm, as shown in table I. The output from each thermocouple was recorded once every 5 sec during the initial cooling and once per second during cooling and solidification near the eutectic temperature. Thus, data points in figures 5(b) and (d) are 1 sec apart. Repeated cycling in the BUF did not increase the undercooling.

A larger variety of cooling rates and thermal gradients could be obtained in the glove box furnace. Ingots could be positioned at different locations in the furnace to obtain different thermal gradients. They could be easily removed and cooled in different ways, giving a variety of different cooling rates and thermal gradients if desired. In this way, cooling rates were varied between 0.04 and 4.1 K/sec. An effort was made to keep the thermal gradient constant at about 3.5 K/cm; however, at the higher cooling rate the gradient was as high as 6.9 K/cm, table I. Figure 6 shows a typical temperature time profile of a slowly cooled undercooling experiment in the glove box. The glove box was continuously kept at a positive pressure of argon. Thermocouple leads were fed through a sealed fitting to a Traveling Data Logger which used the same computer hardware and similar software as that used with the BUF.

Undercooling and Solidification Procedure

The cleaning and conditioning procedures used for the different ingots varied depending on the undercooling desired. Samples in which high undercoolings were desired were thermally cycled in the glove box. During the soak of each cycle, ingots were thoroughly mixed with oil (Dow Corning 704). A glass sleeved thermocouple was used to stir the molten bath. The used oil was decanted after each solidification cycle. The undercooling achieved increased

with each cycle until it reached its maximum value in the third or fourth cycle. The undercooling was defined as the difference between the liquidus, obtained from the phase diagram at the composition prepared (fig. 2), and the lowest temperature attained before the heat of recalescence began to increase the temperature of the sample. Solid impurities present in the bath are believed to serve as heterogeneous nucleation sites and limit undercooling. Evidence of impurities being removed from the bath during the above process are twofold. First, the silicone oil used to cover the melt is very pure, clear, and stable at the temperatures used. This oil becomes black and cloudy during the first cycle and less dirty after subsequent cycles. The second evidence of impurity removal is the increase in undercooling with each melt/mix/solidify cycle. A series of chemical analyses of the dirty oil revealed only trace amounts of Pb and Sn and no trace of the following elements to the limits of detection: Al, Ca, Cd, Co, Cr, Cu, Fe, Li, Mg, Mn, Mo, Na, Ni, Si, Ti, W, Zn, and Zr. Residual lead and tin oxides on the surface of the shot material are believed to be the source of the trace Pb and Sn found in oil. Oxides on the surface of the shot break up after melting and float to the melt-oil interface where they are coated by the oil and then decanted when the oil is changed after the solidification cycle. After the second cycle the oil again appears dirty but not as dirty as after the preceding cycle. The oil is clean and clear after completion of the fourth cycle indicating that most of the impurities removable by this method have been extracted. Chemical analysis of ingots after cycling has shown that their composition is not affected by the process.

Samples in which small undercoolings were desired were not cycled and were solidified with the original oil in which they were stirred. When still less undercooling was desired, Cu powder (0.06 mm diam) was used to nucleate the alloy. The Cu powder was added to the bath during cooling, at a temperature of 220 °C. The powder sat on the surface, coating the outside of the ingot; no Cu particles were found in the bulk of the solidified sample after sectioning. In one sample, a stainless steel screen (50 mesh) was held at the approximate center of the bath, the plane of the screen perpendicular to gravity. This screen experiment helped to clarify certain aspects of the proposed sedimentation process. The procedure used for each experiment is briefly summarized in table I.

The undercooled and solidified samples were cut longitudinally down the center, mounted in metallographic epoxy and polished for metallographic and microprobe analyses. Compositions of the different phases were measured using microprobe wave length dispersive analysis. The electron beam of the microprobe was either swept across the sample obtaining an area raster or focused to a diameter $\approx 0.5 \mu\text{m}$ and scanned normal to a set of dendrites to yield a point of line probe analysis. The microprobe was calibrated using pure Pb and Sn standards.

RESULTS

In table I, the undercooling, cooling rate, thermal gradient just prior to nucleation, and a brief summary of the experimental procedure are presented. A small positive thermal gradient is present from bottom to top, with the top being hotter than the bottom prior to nucleation. Undercooling at the bottom is thus somewhat larger than at the top. The undercoolings listed are those recorded by the bottom thermocouple. The minimum and maximum undercoolings at the extreme top and bottom of the ingot can be estimated by assuming a linear

thermal gradient. For example, the ingot with a thermal gradient of 6.9 K/cm (number 4) had an estimated undercooling of about 6 K at the very top and 24 K at the very bottom. Only one thermocouple was used in ingot number 5; the thermal gradient was estimated to be that of the average of the other slow cooled samples. Since the thermocouple which measured the undercooling (18.5 K) was 1.5 cm above the bottom, the maximum undercooling in this sample is probably closer to 23 K.

In table II, three of the ingots of this study (numbers 6 to 8) are compared to the results obtained by Hollomon and Turnbull (ref. 4), Sundquist and Mondolfo (ref. 5), and Chu et al. (ref. 7) for the same compositions. All of the referenced undercoolings were obtained in small, droplet sized samples, either through use of an emulsification technique (ref. 7), or a hot stage microscope (refs. 4 and 5). The thermal and microstructural data of this study imply that the primary phase in the undercooled eutectic ingots is the lead-rich phase. This is supported by the observations of Chu et al. and others (refs. 4, 5, and 7) who noted two distinctly separate nucleation events in the eutectic alloy. In the study by Chu et al., the lead-rich phase nucleated first with a small undercooling (21 °C below the eutectic) and was then followed by nucleation of the tin-rich phase at a much lower temperature. In the eutectic ingot number 6 it is believed the secondary phase nucleated after the recalescence caused by primary phase solidification, at a temperature close to 182 °C. Due to the effects of variations in composition, which develop rapidly during solidification, the actual undercooling of the secondary phase in the eutectic ingot number 6 may be closer to ≈ 10 °C. During solidification the composition near the top of the eutectic ingot became close to 70 wt % Sn with a liquidus of about 193 °C.

After nucleation of the primary phase, with some undercooling, the remaining liquid may also undercool below the eutectic temperature (183 °C) if the primary phase does not nucleate the secondary phase very well. This is the situation in the Pb-12.5 wt % Sn samples of both Hollomon and Turnbull, and this study. Others, such as Sundquist (ref. 5), define this undercooling as the difference between the nucleation temperature and the secondary phase liquidus at the enriched composition given by the extended primary phase liquidus, rather than the difference between T_n and the eutectic temperature, as in this study. On the other hand, when the primary phase is tin-rich, the remaining liquid does not undercool, as shown by the data for the hypereutectic, tin rich samples (Pb-77 wt % Sn). This suggests that the tin-rich phase nucleates the lead-rich phase effectively.

In figures 7 to 14, photomicrographs of the longitudinal cross sections and composition measurements of the samples listed in table I are shown. The compositions shown were obtained using microprobe area rasters of approximately 0.1 by 0.1 mm. The microprobe measurements were normalized so that the average composition after normalization was equal to the initial alloy composition. The data were normalized by multiplying each value by the ratio of the actual, as weighed composition of the alloy to the average of the measured data, that is: $\text{normalized datum} = \text{measured datum} \times (\text{actual average composition} / \text{measured average composition})$. The average of the raw, not normalized, microprobe composition measurements are included in table III.

The composition variations in the top and bottom half regions of ingots numbers 6 to 8 measured using the microprobe were checked for accuracy using

the wet chemical analysis technique Atomic Absorption Spectrophotometry (table IV). The ingots were sectioned such that the filings from the top half of the ingots were saved and labeled and then the bottom half of the ingots were cut and the filings saved. The average compositions of the top and bottom halves of the ingots determined by the microprobe are in agreement with the results of the chemical analysis. Relative accuracies of the chemical analyses are ± 5 percent for ingots numbers 6 and 8, and ± 10 percent for ingot number 7.

Figure 7 shows the longitudinal cross section of the slow cooled sample (number 1) in which Cu powder was used to nucleate the bath and minimize undercooling. A few Pb-rich dendrites are seen at the very bottom of this sample. The rest of the sample is void of dendrites. The microstructure indicates predominately lamellar eutectic and, in some areas, nonlamellar eutectic. Grains of eutectic can be seen growing vertically up, directionally, in the top two-thirds of the sample. The segregation in this sample, undercooled 4.2 K, is limited to local variations, as shown by the composition measurement in figure 7. The average value is very nearly the starting composition, indicating no significant macrosegregation. The Pb-rich dendrites at the sample bottom do not significantly affect the average composition.

The structural and compositional variations of ingot number 2 are shown in figure 8. Spherical, cylindrical, and cross (+) shaped Pb-rich dendritic particles, surrounded by eutectic, are randomly arranged in the bottom of the ingot. No Pb-rich dendrites are present in the top half of the sample. The eutectic grains above the Pb-rich dendrites are believed to have grown upwards (after nucleation and growth of the Pb-rich dendrites), in the direction of the thermal gradient which remained after recalescence. No clear indication exists of macrosegregation from the composition measurements shown in figure 8. However, the six measurements taken in the bottom region, which contained the Pb-rich dendrites, indicated an average composition of Pb-58 wt % Sn. The lower portion of the ingot is thus slightly richer in Pb than the equilibrium eutectic.

Figure 9 shows the structure and composition measurements of ingot number 3, the slow cooled ingot which was thermally cycled and undercooled 20.6 K prior to nucleation. The top one-third of this ingot consists of grains of primarily ordered groups of Sn-rich dendrites and interdendritic eutectic. In the approximate center of the ingot are columnar grains of eutectic free of Pb and Sn-rich dendrites. On the right-hand side of the ingot a eutectic solidification front can be seen which grew up from the bottom region. Eutectic grains also grew down from the grains of Sn-rich dendrites above, to form a eutectic grain boundary at which the two fronts met. It is also apparent that the right-hand side of the ingot, near this eutectic region, was pulled away from the tube wall due to shrinkage. This shows that the dendrite free eutectic areas in the approximate center of the ingot were last to solidify. In the bottom one-half of the sample, Pb-rich dendrites are located with a considerable amount of eutectic. The composition measurements of figure 9 clearly show the macrosegregation. The average composition at the top is about Pb-68% Sn while the composition at the bottom is approximately Pb-58% Sn.

The oil quenched and thermally cycled sample, ingot number 4, is shown in figure 10. This sample was undercooled about the same amount as ingot number 3. However, the cooling rate just prior to nucleation was about 100 times faster. The bottom one-third of the ingot contains the round, rod, and cross shaped Pb-rich dendrite fragments characteristics of the other samples. The

volume fraction of Pb-rich dendrites to eutectic is greatest at the very bottom and decreases toward the center. The top one-third of the ingot consists of grains of Sn-rich dendrites and eutectic. In the center of the ingot are blossoming grains of eutectic which resemble those of an equiaxed zone. The composition measurements shown in figure 10 indicate this sample to be the most severely segregated. The average compositions at the top and bottom are about Pb-72% Sn and Pb 55% Sn respectively.

Figure 11 shows the structure of ingot number 5, the Pb-Sn eutectic ingot, undercooled 20 K and solidified with a stainless steel screen held near the center. The macrosegregation process in this sample is very similar to that proposed for the two previously discussed ingots, but the screen has not permitted the Pb-rich dendrites which formed near the top of the sample to settle to the bottom.

In figure 12 the macrostructures of ingot number 6 is shown. This ingot is similar to the other highly undercooled ingots, lead-rich dendrites at the bottom of the ingot, a primarily lamellar eutectic structure in the middle, and tin-rich dendrites and eutectic at the top. The higher amount of undercooling and intermediate cooling rate have not significantly affected the segregation found in this ingot. The Pb-12.5 wt % Sn alloy (ingot number 7) has a uniform distribution of lead-rich dendrites and a small amount of interdendritic eutectic throughout the sample. The Pb-77 wt % Sn ingot (number 8) consists of tin-rich dendrites and eutectic; only relatively small amounts of macrosegregation are observed in these ingots. Figures 13 and 14 show the macrostructure and variation of composition along the length of these ingots.

The average dendrite and eutectic compositions of ingots numbers 6 to 8 are shown in table V. Figure 15 is a SEM back scattering photomicrograph of an interdendritic eutectic area in the Pb-12.5 wt % Sn sample. As shown in table V, microprobe analysis of this eutectic area indicates an average composition of Pb-89 wt % Sn. The area analyzed to obtain this result was within the Sn-rich phase of the eutectic, thus did not include the eutectic, rich in Pb, in contact with the dendrites. For this reason, the actual composition of the remaining liquid of the Pb-12.5 wt % Sn alloy is believed to be slightly less rich in tin than what was measured. The lead-rich dendrites in this sample were found to have an average composition of about 10 wt % Sn.

Since the composition varies widely over the length of the undercooled eutectic ingots, dendrite and eutectic composition measurements were made at the top, middle, and bottom regions of ingot number 6 as reported in table V. Chu et al. (ref. 7) reported energy dispersive x-ray analysis on their eutectic sample listed in table II. It was determined that the tin-rich phase was approximately 80 wt % Sn and the lead-rich phase about 10 to 20 wt % Sn.

Microsegregation in the Pb-77 wt % Sn alloy (ingot number 8) was analyzed using microprobe beam scans perpendicular to the dendrites and area rasters of the interdendritic regions (fig. 16). The average of both the area rasters and point analyses in the interdendritic regions is about Pb-62 wt % Sn. The average of the point analyses within the tin-rich dendrites is 99 wt % Sn.

DISCUSSION

Nucleation

The thermal measurements indicate that in the Pb-12.5 wt % Sn ingot (number 7) primary nucleation of the Pb-rich phase occurs at an undercooling of 12 K below the liquidus. Nucleation of the Sn-rich phase (when the interdendritic liquid was enriched to the normal and hyper-eutectic compositions), on the other hand, occurred with an undercooling of 20 °C below the eutectic temperature. Since the cooling rate is fairly slow (≈ 1 K/sec), local equilibrium is assumed. Thus, during cooling, solid phases will have a liquid interface temperature and composition given by the phase diagram and undercooled phases by metastable extensions of liquidus and solidus. The composition of the interdendritic liquid thus follows the α -liquidus line of the phase diagram. The composition of the undercooled liquid in contact with the dendrites is expected to be indicated by the extended α -liquidus. Solidification of this undercooled interdendritic liquid produced the eutectic structure, supersaturated with Sn with respect to the equilibrium eutectic, shown in figure 15 and table V.

The development of the morphology of the Pb-12.5 wt % Sn ingot (number 7), as confirmed by the thermal measurements, appears to be similar to that proposed by Chu et al. for emulsified droplets containing less than 80 wt % Sn. The lead-rich dendrites nucleate first at some temperature below the α -liquidus and grow. Growth of the α -phase occurs during recalescence and subsequently as the alloy cools to some temperature below the eutectic temperature. The tin-rich eutectic phase then nucleates and grows. The measurements in this study indicate the peak recalescence temperature of the α -phase was significantly below the equilibrium liquidus temperature, as shown in table II. Similarly, after the second nucleation event, the recalescence temperature is less than the equilibrium eutectic temperature. The macrosegregation observed in the eutectic alloy of this study was not apparent in the work by Chu et al. because of the small size of the emulsified droplets.

The effect of undercooling on the composition and structure of the eutectic is emphasized by comparing the undercooled Pb-12.5 wt % Sn and not undercooled Pb-77 wt % Sn interdendritic regions of ingots (numbers 7 and 8). The eutectic in the lead-rich sample was not lamellar but consisted of nearly pure tin (β -phase) with irregular particles of lead-rich, α -phase. This mixture had a measured composition of Pb-89 wt % Sn. The structure of the eutectic in the Pb-77 wt % Sn ingot was primarily lamellar, with a measured composition of Pb-62 wt % Sn. Similar eutectic structures, supersaturated with tin, were obtained by Chu et al. in lead-rich and near-eutectic alloys (ref. 7).

In the Pb-77 wt % Sn ingot (number 8), the solidification of the primary phase again occurred with a peak recalescence temperature well below the liquidus for the initial composition. The data in figure 5 show this; the liquidus of the alloy is 202 °C and the peak recalescence temperature is only about 190 °C. The nucleation temperature of the Sn-rich phase was 12 °C below the eutectic temperature. Thus, the first solid to form should have a composition given by the metastable extension of the β -liquidus. One might then expect the center of the Sn-rich dendrites to be supersaturated with lead. However, a simple energy balance indicates that less than 10 wt % of the liquid will solidify during recalescence. The areas which are initially supersaturated with lead become obscured as a result of solid state diffusion processes.

The enriched interdendritic liquid of the Pb-77 wt % Sn ingot did not undercool; however, there was a large amount of undercooling before secondary phase nucleation in the Pb-12.5 wt % Sn ingot (tables I and II). Eutectic liquid undercooled when in contact with Pb-rich dendrites, but did not in the presence of Sn-rich dendrites, indicating that Pb is a poor nucleant for Sn but that Sn is an effective nucleant for Pb. This type of nucleation behavior is termed nonreciprocal. As discussed earlier (see pp. 3-6, fig. 1 and appendix A), theory predicts this for the Pb-Sn system. Because the solid-liquid interfacial energy of Sn is more than two times that of Pb, the nucleation barriers associated with the nucleation of Pb are hundreds of orders of magnitude less than those for the nucleation of Sn.

In agreement with the above mentioned theory, the thermal data and microstructures of this study indicate that in the undercooled eutectic alloys, lead-rich dendrites nucleate and grow first, as shown in table II. Consequently the remaining liquid becomes richer in tin and thus promotes subsequent growth of a tin-rich, off eutectic, lamellar structure, and the growth of tin-rich dendrites. Figures 17(a) and (b) show the microstructures from two different areas of the undercooled eutectic ingot number 6. No indication of lead-rich dendrites nucleating the eutectic was evident in the microstructure; conversely, the eutectic is often observed radiating from tin-rich dendrites. This gives additional experimental evidence of nonreciprocal nucleation behavior. The results thus confirm the findings of Sundquist and Mondolfo (ref. 5) concerning nonreciprocal nucleation and extend them to bulk sized samples.

Macrosegregation

Given sufficient undercooling, the Pb-rich dendritic phase is the primary phase in the Pb-Sn eutectic ingots. The extent of (Pb-rich) dendrite solidification depends on the amount of undercooling prior to the first nucleation event; the fraction of Pb-rich dendrites formed is higher at higher undercoolings. With higher undercoolings and more Pb-rich dendrites, the liquid becomes more rich in Sn. With liquid compositions more rich in Sn at higher undercoolings, extensive remelting of the Pb-rich dendrites appears to take place.

The experimental observations may be explained on the basis of the above hypothesis. Thus, in ingot number 1, which has a small undercooling, only a small amount of Pb-rich dendritic solidification took place and no significant macrosegregation. The composition of the solidifying two phase solid is nearly the same as the liquid. The maximum undercooling in ingot number 1, about 6 K, was just enough to drive the small amount of metastable Pb-rich dendritic solidification observed.

A greater fraction of Pb-rich dendrites occurs with undercoolings of 8 K or more, as in ingots numbers 2 to 5. At these undercoolings, dendrite tip velocities, estimated from earlier measurements by others, are of the order of at least a few centimeters per second (refs. 16, 21, and 22). This would allow the rapid growth of a dendritic skeleton across the highly undercooled portion of the ingot. However, dendritic remelting, occurring during and immediately following recalescence, fragments this skeleton which breaks into spherical, cylindrical, and cross (+) shaped dendritic particles (refs. 18 and 23). These fragments then settle to the bottom causing macrosegregation.

No indication of buoyancy driven convection in the liquid state was observed in this study. It is likely in ingot number 2 that the Pb-rich dendrites grew only in the bottom half of the ingot, the portion of the ingot undercooled at least 5 K. This alone would not result in any macrosegregation. For macrosegregation to develop, movement of the now Sn-rich liquid up, and/or the Pb-rich dendrites down, is required. Since the density difference between the solid and liquid phase is much greater than those in the liquid because of composition and temperature gradients in the liquid, the settling of the solid dominates. This is shown in the composition variation of ingot number 2, fig. 8. The Pb-rich dendrites which grew in the bottom half of the ingot sank to the bottom fifth, leaving the liquid above richer in Sn as shown.

A number of experiments examined the convection and segregation in the liquid. The mid-ingot screen of number 5 was designed to stop solid sedimentation and not significantly impede segregation in the liquid. During the time the bath is undercooled (about 3 min in the slowly cooled ingots) it is possible that clusters of Pb and/or Sn atoms form and sink and float respectively. If this were to occur to a significant extent, a channel of Pb-rich and/or Sn-rich material would be seen at the edges of the screen; this is not the case as seen in figure 11. Ingot number 5 also shows that Pb-rich dendrites can grow throughout the bath and that the segregation is rather insensitive to the small gradients of these experiments. To prevent any segregation in the liquid, the liquid was vigorously stirred prior to cooling. In another experiment, during the final stages of cooling below the eutectic temperature, a small amount of liquid was removed from the top using a small ladle. This liquid was chemically analyzed and found to be of eutectic composition, thus indicating no segregation in the liquid prior to nucleation.

With initial undercoolings of about 20 K the volume fraction of Pb-rich dendrites is greater (as compared to ingots solidified with less initial undercooling), thus the composition of the liquid they leave behind after settling is richer in Sn. In the top region of the ingot, the liquid is rich enough in Sn to grow Sn-rich dendrites (see fig. 9). The increase in undercooling from 8 to 20 K increased the amount of macrosegregation.

At faster cooling rates, such as that used to solidify ingot number 4, it is believed that a larger amount of Pb-rich dendrites form during recalescence. The remelt and breakup of the Pb-rich dendrites is thus more extensive because local Sn concentrations are higher. This results in finer Pb-rich dendrite fragments, a greater packing density at the ingot bottom, and an increase in macrosegregation compared to ingot number 3 (figs. 9 and 10).

CONCLUDING SUMMARY

1. Given a sufficient amount of undercooling (≈ 5 K or more), the dendritic Pb-rich phase is the primary phase in the Pb-Sn eutectic alloy. Because of Sn enrichment of the liquid and thermal recalescence, the Pb-rich dendrites which form in the undercooled eutectic ingot remelt and fragment. These fragmented dendrites are then free to sink to the bottom causing segregation.

2. The extent of (Pb-rich) dendritic solidification increases as undercooling increases. As Pb-rich dendrites grow, breakup, and settle to the bottom, the remaining liquid in the upper region of the ingot becomes more rich in Sn. With an undercooling of 20 K, the liquid at the top region of the ingot

is rich enough to grow Sn-rich dendrites. These effects cause greater amounts of macrosegregation as compared to ingots solidified with less undercooling at the same cooling rate. A Pb-Sn eutectic ingot undercooled 20 K with a cooling rate of 4 K/sec just prior to nucleation had a composition of about Pb-72 wt % Sn at the top and 55% Sn at the bottom.

3. The nucleation behavior of the Pb-Sn system is nonreciprocal such that the solid Pb-rich phase does not nucleate the Sn phase well, however, the solid Sn-rich phase does nucleate the Pb phase effectively. This phenomenon is believed to be mainly the result of differences in solid-liquid interfacial energies between the catalyst, new solid, and undercooled liquid rather than lattice misfit between the catalyst and new solid.

4. No channeling or other indications of segregation in the liquid state, because of density gradients in the liquid or clustering of Pb and/or Sn-rich atoms during undercooling, was observed in this study.

APPENDIX A

Calculation of P: the relative probability of nucleating Pb on Sn rather than nucleating Sn on Pb in the undercooled Pb-Sn eutectic alloy.

$$P = \frac{\exp(-16\pi(\gamma_{Pb})^3 f_{Pb} / 3(\Delta S_{Pb} \Delta T)^2 kT)}{\exp(-16\pi(\gamma_{Sn})^3 f_{Sn} (\Delta S_{Sn} \Delta T)^2 kT)}$$

$$\gamma_{Pb} = 56 \text{ erg/cm}^2 = 56 \times 10^{-7} \text{ J/cm}^2$$

$$\gamma_{Sn} = 132 \times 10^{-7} \text{ J/cm}^2 \text{ (ref. 9)}$$

Assuming a contact wetting angle for the nucleating Pb cap of 10° , and a resultant angle of 100° calculated for the Sn cap, the values for the factor, f , decreasing the nucleation barrier due to heterogeneous nucleation, are

$$f_{Pb} = (2 + \cos 10^\circ)(1 - \cos 10^\circ)^2 / 4 = 1.72 \times 10^{-4},$$

$$f_{Sn} = 0.616.$$

Assuming the entropy of fusion of the solid alloys to be constant and equal to that of the pure components the values of ΔS_f are (ref. 12),

$$\Delta S_{Pb} = \Delta H_{Pb} / T_m = (6.26 \text{ cal/g}) / 11.34 \text{ g/cm}^3 / 600 \text{ K} = 0.118 \text{ cal/cm}^3 \text{ K}$$

$$\Delta S_{Pb} = 0.495 \text{ J/cm}^3 \text{ K}$$

$$\Delta S_{Sn} = 0.877 \text{ J/cm}^3 \text{ K}$$

$$k = 1.38 \times 10^{-23} \text{ J/K}$$

Now calculating P, the probability ratio, at an undercooling of 20 K ($\Delta T = 20 \text{ K}$, $T = 436 \text{ K}$),

$$P = \exp(-0.858) / \exp(-1.4 \times 10^4) = 0.424 / < 10^{-500}$$

Thus theory predicts that the Pb phase of the Pb-Sn eutectic is extremely more likely to nucleate on Sn than the Sn phase of the eutectic heterogeneously nucleating on Pb, at 20 K undercooling.

To determine the relative likelihood of homogeneous nucleation of Pb eutectic solid or Sn eutectic solid we may simply remove the factor, f , from the ΔG_n equation. This probability ratio, P_{hom} , at an undercooling of $0.3T_m = 137 \text{ K}$ is

$$P_{hom} = \exp(-145) / \exp(-663) = 9 \times 10^{224}$$

This indicates there is an extremely greater probability of Pb nucleating rather than Sn. Again theory is in agreement with experimental observations predicting Pb to be the primary phase of the eutectic (refs. 7, 13, and 14).

APPENDIX B

Notes concerning calculation of the density difference between Pb-rich dendrites and eutectic liquid.

Pb dendrites are 19.2 wt % Sn, or 27 vol % Sn

Liquid eutectic is 61.9 wt % Sn, or 71.6 vol % Sn

Density of Pb dendrite = $11.34(1 - 0.27) + 7.3(0.27) = 10.2 \text{ g/cc}$

Density of the liquid eutectic = $(11.34(1 - 0.716) + 7.3(0.716))0.97 = 8.2 \text{ g/cc}$

REFERENCES

1. Chalmers, B.: Principles of Solidification. R.E. Krieger Pub., 1964, pp.213-224.
2. Heine, R.W.; Loper, C.R.; and Rosenthal, P.C.: Principles of Metal Casting, 1955, McGraw-Hill, pp. 298, 491.
3. Allen, B.C.; and Isserow, S.: Segregation at the Eutectic Temperature. Acta Met., vol. 5, no. 8, Aug. 1957, pp. 465-472.
4. Hollomon, J.H.; and Turnbull, D.: Solidification of Pb-Sn Alloy Droplets. J. Met., vol. 3, no. 9, Sept. 1951, pp. 803-805.
5. Sundquist, B.E.; and Mondolfo, L.F.: Heterogeneous Nucleation in the Liquid-to-Solid Transformation in Alloys. Trans. Met. Soc. AIME, vol. 221, no. 1, Feb. 1961, pp. 157-164.
6. Perepezko, J.H.; and Paik, J.S.: Undercooling Behavior of Liquid Metals. Rapidly Solidified Amorphous and Crystalline Alloys, MRS Symp. Proc. Vol. 8, B.H. Kear, B.C. Giesser, and M. Cohen, eds., Materials Research Society, 1982, pp.49-64.
7. Chu, M.G.; Shiohara, Y.; and Flemings, M.C.: Solidification of Highly Undercooled Sn-Pb Alloy Droplets. Metall. Trans. A, vol. 15, no. 7, July 1984, pp. 1303-1310.
8. Turnbull, D.: Formation of Crystal Nuclei in Liquid Metals. J. Appl. Phys., vol. 21, no. 10, Oct. 1950, pp. 1022-1028.
9. Gunduz, M.; and Hunt, J.D.: The Measurement of Solid-Liquid Surface Energies in the Al-Cu, Al-Si and Pb-Sn Systems. Acta Met., vol. 33, No. 9, 1985, pp. 1651-1672.
10. Porter, D.A.; and Easterling, K.E.: Phase Transformations in Metals and Alloys. Van Nostrand Reinhold Pub., 1981, pp. 191-194.
11. Boyer, H.E.; and Gall, T.L., eds: Metals Handbook, Desk Edition, American Society for Metals, 1985, pp. 1.44-1.48.
12. Youdelis, W.V.; and Iyer, S.P.: Secondary Supercooling in Binary Eutectic Alloy Systems. Met. Sci., vol. 9, 1975, pp. 289-290.
13. de Groh, H.C. III; and Laxmanan, V.: Bulk Undercooling, Nucleation and Macrosegregation of Pb-Sn Alloys. Metall. Trans A, vol. 19, no. 11. Nov. 1988, pp. 2651-2658.
14. de Groh, H.C. III; and Laxmanan, V.: Macrosegregation in Undercooled Pb-Sn Eutectic Alloys. Solidification Processing of Eutectic Alloys, D.M. Stefanescu, G.J. Abbaschian, and R.J. Bayuzick, eds., The Metallurgical Society, Warrendale, PA, 1988, pp. 229-242.
15. Davis, K.G.; and Fryzuk, P.: Grain Structure and Solute Segregation in Bismuth Ingots Solidified from Undercooled Melts. Trans. Met. Soc. AIME, vol. 233, no. 11, Nov. 1965, pp. 1983-1986.

16. Powell; G.L.F., et al.: The Growth Rate of Dendrites in Undercooled Tin. Metall. Trans. A, vol. 8, no. 6, June 1977, pp. 971-973.
17. Kattamis, T.Z.; and Mehrabian, R.: Highly Undercooled Alloys: Structure and Properties. J. Vac. Sci. Technol., vol. 11, no.6, Nov./Dec. 1974, pp. 1118-1122.
18. Kattamis, T.Z.; and Flemings, M.C.: Dendrite Structure and Grain Size of Undercooled Melts. Trans. Met. Soc. AIME, vol. 236, no. 11, Nov. 1966, pp. 1523-1532.
19. Tewari, S.N.: Effect of Undercooling on the Microstructure of Ni-35 At. Pct Mo (Eutectic) and Ni-38 At. Pct Mo (Hypereutectic) Alloys. Metall. Trans. A, vol. 18, no. 4, Apr. 1987, pp. 525-255.
20. Johnson, M.H.; and Griner, C.S.; Compositional Variations in the Undercooled Pb-Sn Eutectic Solidified at Various Acceleration Levels. Scripta Met., vol. 11, no. 3, Mar. 1977, pp. 253-255.
21. Kobayashi, K.; and Shingu, P.H.: Growth Rate of Crystal Nucleated from the Undercooled Melt. Proceedings of the 4th International Conference on Rapidly Quenched Metals, Sendai, Japan, vol. 1, T. Masumoto and K Suzik, eds., Japan Institute of Metals, 1981, pp. 103-106.
22. Orrok, G.T.: Dendritic Solidification of Metals. Doctoral Thesis, Harvard University, 1958.
23. Flemings, M.C., et al.: Dendritic Growth of an Undercooled Nickel-Tin Alloy. Undercooled Alloy Phases, E.W. Collings and C.C. Koch, ed., The Metallurgical Society, Warrendale, PA, 1987, pp. 321-343.

TABLE I. - THERMAL DATA OF UNDERCOOLED Pb-Sn INGOTS

Ingot number	Description	Ingot composition wt % Sn	Undercooling, K	Cooling rate, K/sec	Thermal gradient, K/cm
1	Slow cool, nucleated with Cu powder	61.9 ↓	4.2	0.066	4.4
2	Slow cooled		8.0	0.040	3.2
3	Slow cooled, thermally cycled		20.6	0.042	2.6
4	Oil quenched, thermally cycled		20.8	4.1	6.9
5	Slow cooled, thermally cycled, solidified with s.s. screen		18.5	0.1	3.4 est
6	BUF, furnace quenched		↓	34	0.5
7	BUF, furnace quenched, primary phase Pb	12.5	12	1.1	0.45
7	Secondary phase	12.5	20	0.74	3.6
8	BUF, furnace quenched, primary phase Sn	77	31	0.79	7.5
8	Secondary phase	77	None	0.28	5.1

TABLE II. - COMPARISON OF UNDERCOOLING MEASUREMENTS OF THOSE FOUND IN THE LITERATURE AND IN INGOTS NUMBERS 6 TO 8 [All temperatures are given in degrees Celsius.]

Authors	Primary phase	Composition wt % Sn	Undercooling, nucleation and peak recalescence temperature of primary phase			Undercooling, nucleation and peak recalescence temperature of secondary phase		
			UC	T _n	T _r	UC	T _n	T _r
This study	Pb	12.5	12	285.7	288.8	20	163.3	164.6
Hollomon and Turnbull (ref. 4)	Pb	12.5	40	256	-----	13	170	-----
This study	Pb	61.9	34	148.7	181.7	1	182	183.7
Hollomon and Turnbull (ref. 4)	Pb	^a 61.9	43	140	-----	-----	-----	-----
Chu, Shiohara, and Flemings (ref. 7)	Pb	61.9	21	162	-----	60	162	-----
This study	Sn	77	31	170.9	189.1	None	-----	-----
Sundquist and Mondolfo (ref. 5)	Sn	77	56	144	-----	None	-----	-----

^aUndercooling extrapolated from data near eutectic composition.

TABLE III. - AVERAGES OF THE RAW, NOT NORMALIZED MICROPROBE COMPOSITION MEASUREMENTS IN wt % Sn

	Ingot number							
	1	2	3	4	5	6	7	8
Raw average composition	63.4	64.0	68.0	63.4	69.1	68.6	15.0	80.1

TABLE IV. - CHEMICAL ANALYSIS OF THE TOP AND BOTTOM REGIONS OF INGOTS NUMBERS 6 to 8 IN wt % Sn

	Ingot number		
	6	7	8
Composition in top half	69.2	12.4	79.8
Composition in bottom half	58.4	12.6	75.6

TABLE V. - DENDRITE AND REMAINING LIQUID MICROPROBE MEASUREMENTS OF COMPOSITION, INGOTS NUMBERS 6 TO 8

Alloy	Lead-rich dendrites wt % Sn	Tin-rich dendrites wt % Sn	Last liquid to solidify wt % Sn
Pb 12.5% Sn	10	--	89
Pb 61.9% Sn (top)	-----	97	66
Pb 61.9% Sn (mid)	-----	--	65
Pb 61.9% Sn (bot)	23	--	74
Pb 61.9% Sn (Chu, ref. 7)	10 to 20	--	80
Pb 77% Sn	-----	99	62

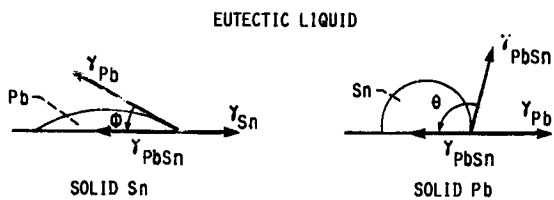


FIGURE 1. - RELATIVE WETTING OF A SOLID SPHERICAL CAP OF Pb ON Sn AND Sn ON Pb.

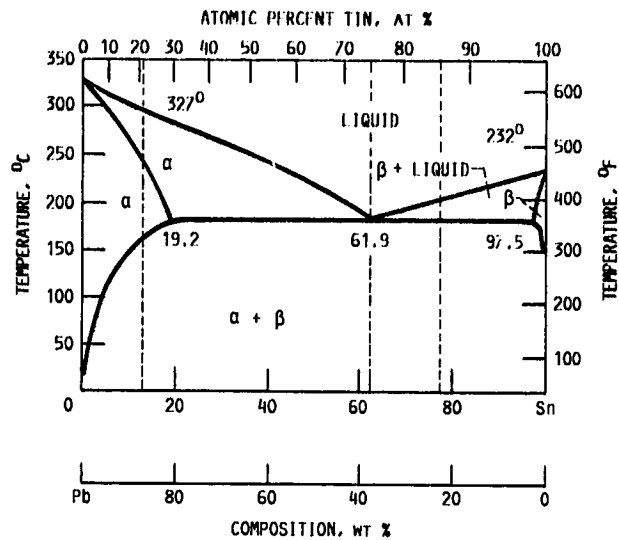


FIGURE 2. - Pb-Sn PHASE DIAGRAM SHOWING THE COMPOSITIONS STUDIED AS DASHED LINES, Pb 12.5 wt % Sn, Pb 61.9% Sn AND Pb 77% Sn.

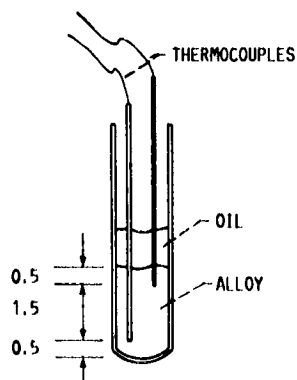


FIGURE 3. - SCHEMATIC OF THE ALLOY INGOT, GLASS CRUCIBLE, AND THERMOCOUPLES. LENGTHS SHOWING LOCATIONS ARE IN MILLIMETERS.

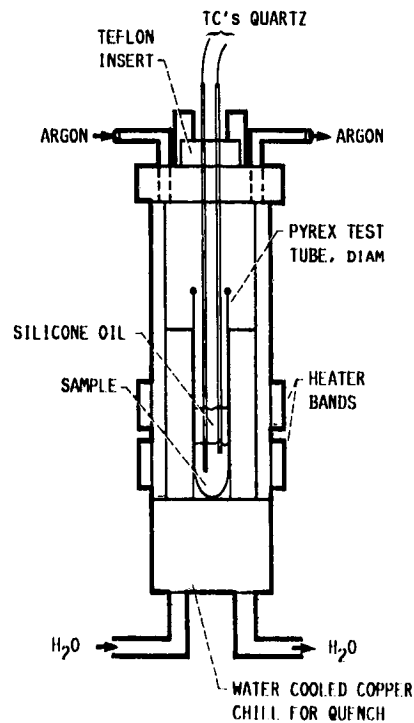


FIGURE 4. - BULK UNDERCOOLING FURNACE (BUF).

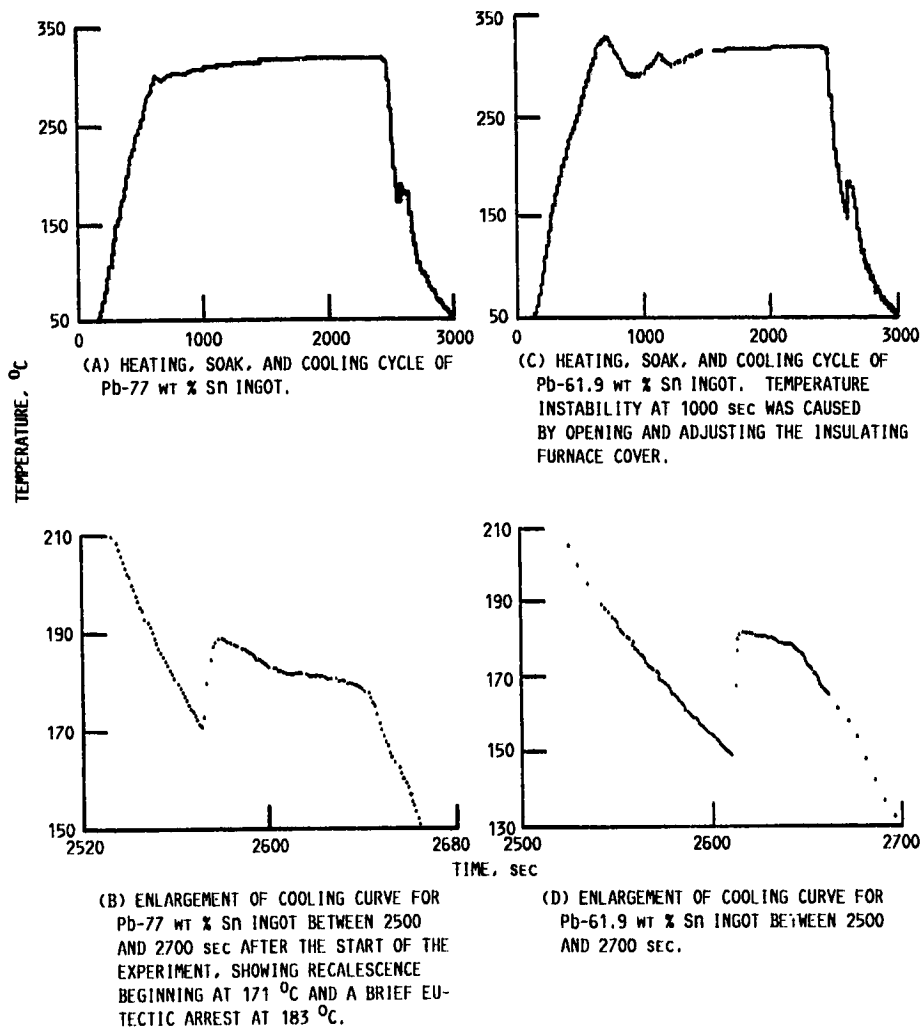


FIGURE 5. - THERMAL DATA FOR THE Pb-77 wt % Sn AND Pb-61.9 wt % Sn INGOTS.

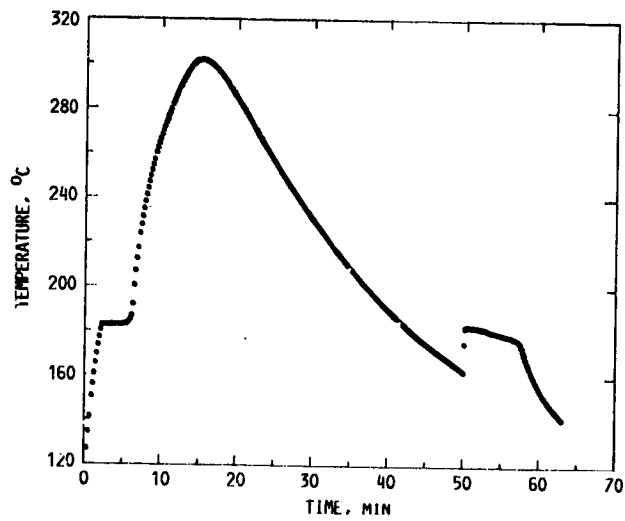
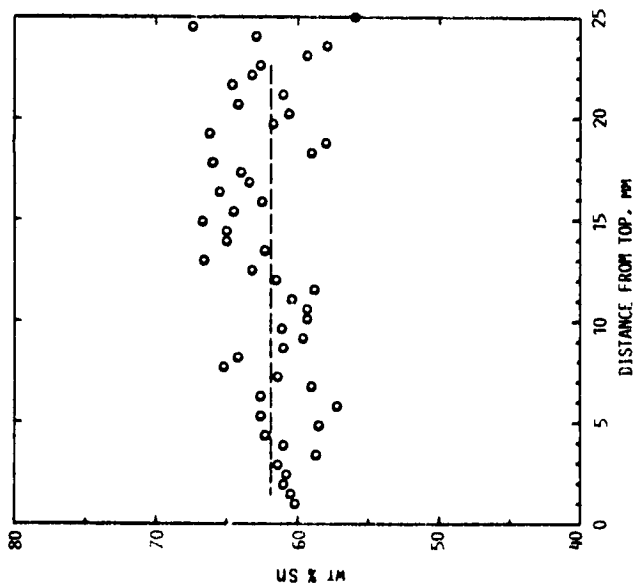
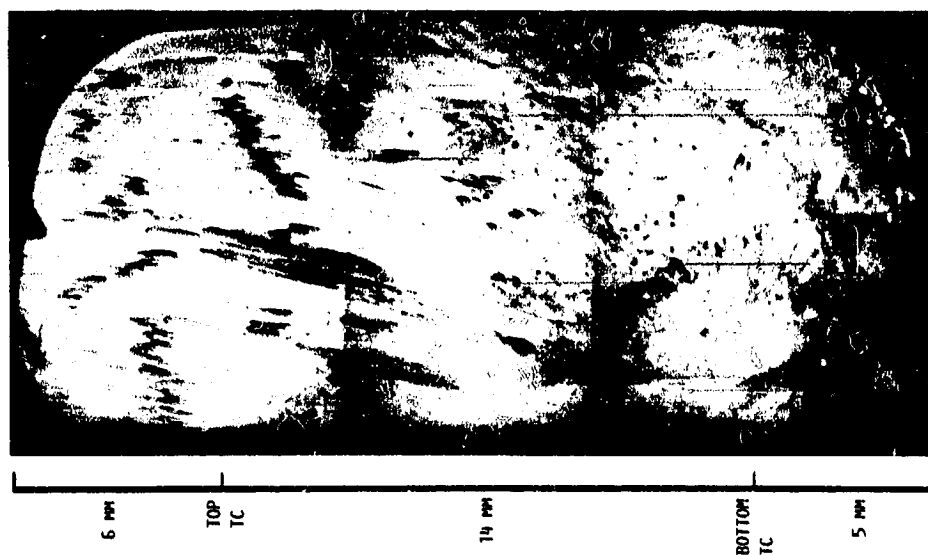
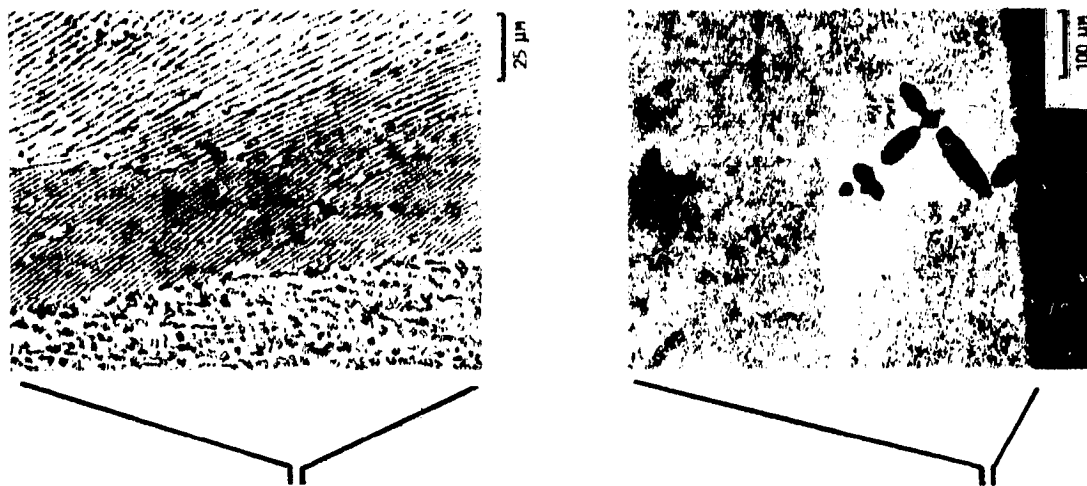
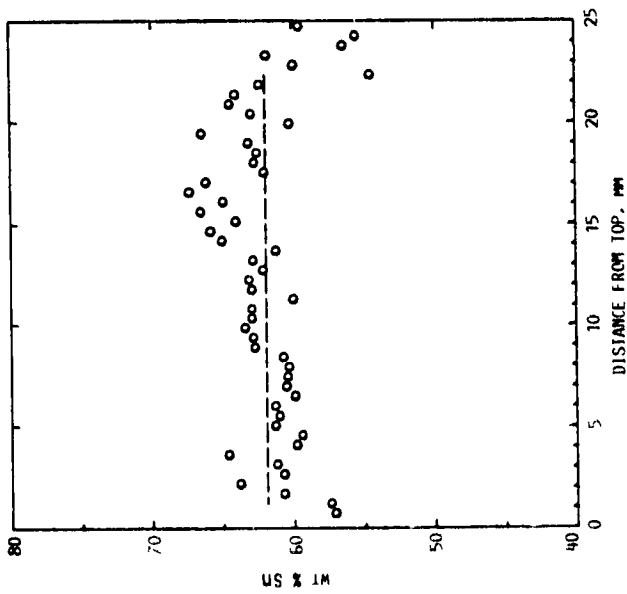


FIGURE 6. - TEMPERATURE-TIME DATA MEASURED BY THE BOTTOM TC OF INGOT NUMBER 3. DATA COLLECTION RATE WAS ONCE EVERY 10 SEC, THEN INCREASED TO ONCE EVERY 5 SEC DURING THE FINAL STAGE OF COOLING. THE TEMPERATURE OF THE PLATEAU DURING MELTING WAS 182.6 °C. THE THERMAL GRADIENT AND COOLING RATES WERE MEASURED JUST BEFORE RECALESCENCE, ABOUT 50 MIN INTO THE EXPERIMENT.

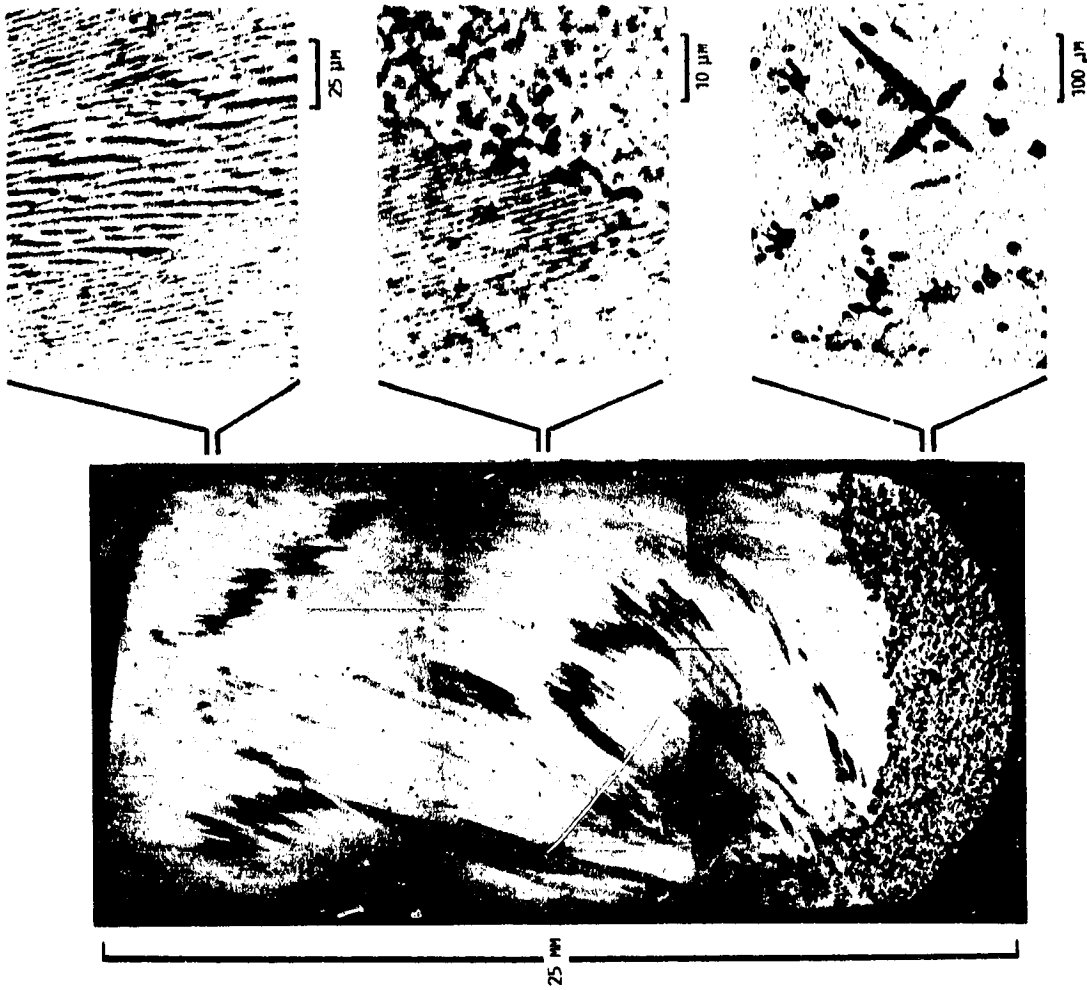


MICROPROBE MEASUREMENTS OF COMPOSITION VARIATIONS OF LONGITUDINAL CROSS SECTION. DASH LINE FOR REFERENCE AT 61.9 PERCENT Sn.

MICROGRAPHS OF LONGITUDINAL CROSS SECTION.
 FIGURE 7. - INGOT NUMBER 1, Pb-Sn EUTECTIC INGOT SLOW COOLED AND NUCLEATED WITH Cu POWDER. $T_{uc} = 4 \text{ K}$.



MICROPROBE COMPOSITION MEASUREMENTS.

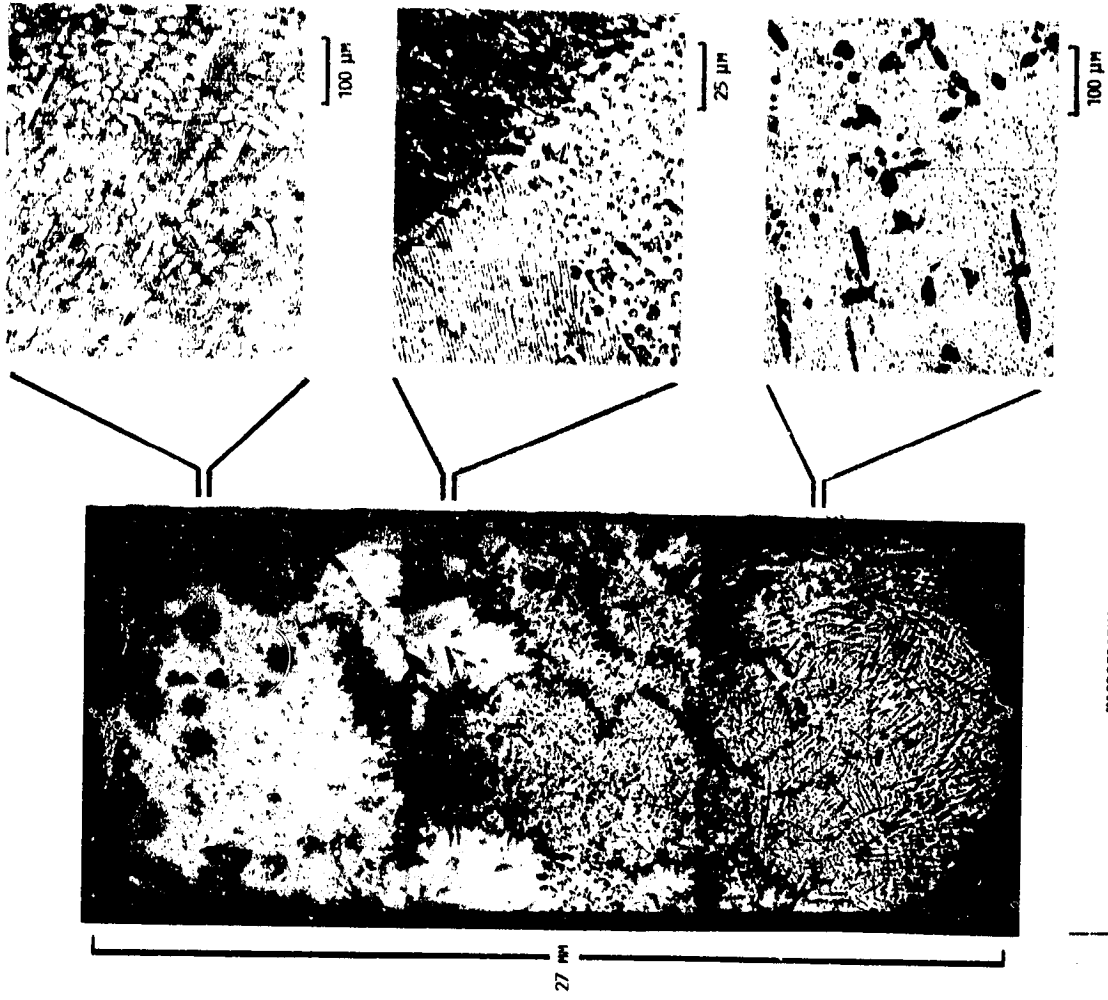


MICROGRAPHS OF LONGITUDINAL CROSS SECTION.

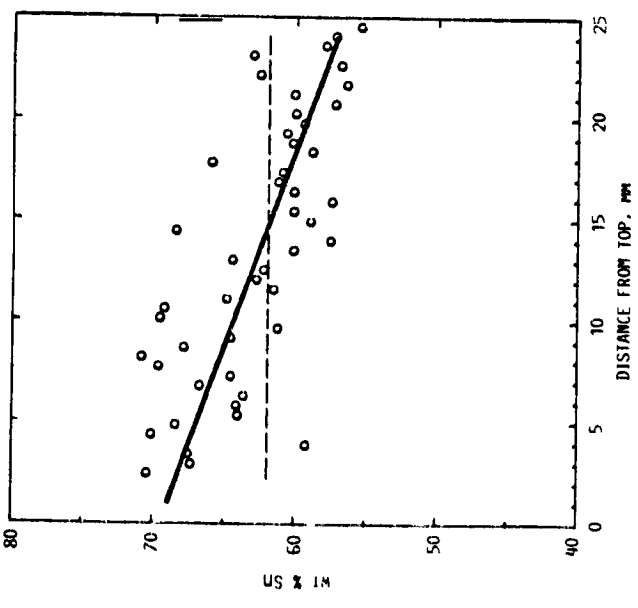
FIGURE 8. - INGOT NUMBER 2, Pb-Sn EUTECTIC INGOT SLOW COOLED, $T_{uc} = 8$ K.

ORIGINAL PAGE IS
OF POOR QUALITY

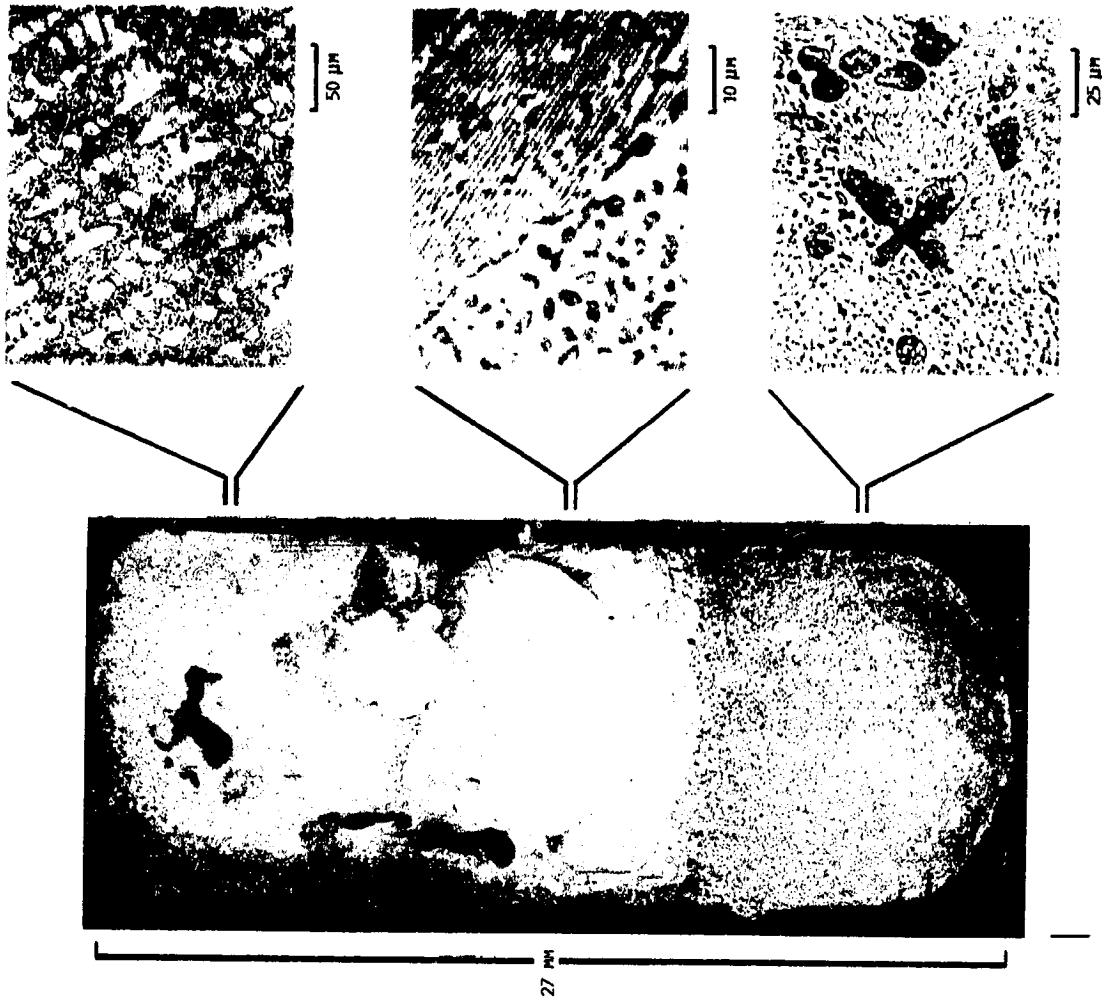
ORIGINAL PAGE IS
OF POOR QUALITY



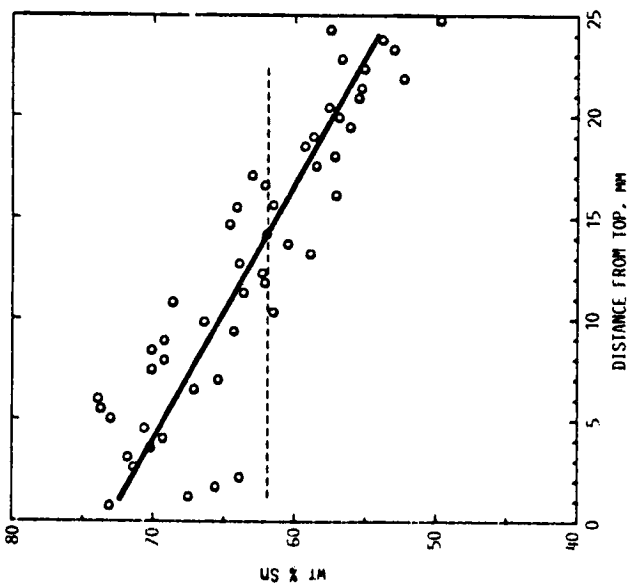
MICROGRAPHS OF LONGITUDINAL CROSS SECTION.
FIGURE 9. - INGOT NUMBER 3, Pb-Sn EUTECTIC INGOT SLOW COOLED AND THERMALLY CYCLED, $T_{uc} = 20$ K.



MICROPROBE COMPOSITION MEASUREMENTS. BOLD LINE IS A
LINEAR REGRESSION. DASH LINE IS FOR REFERENCE AT
61.9 PERCENT Sn.

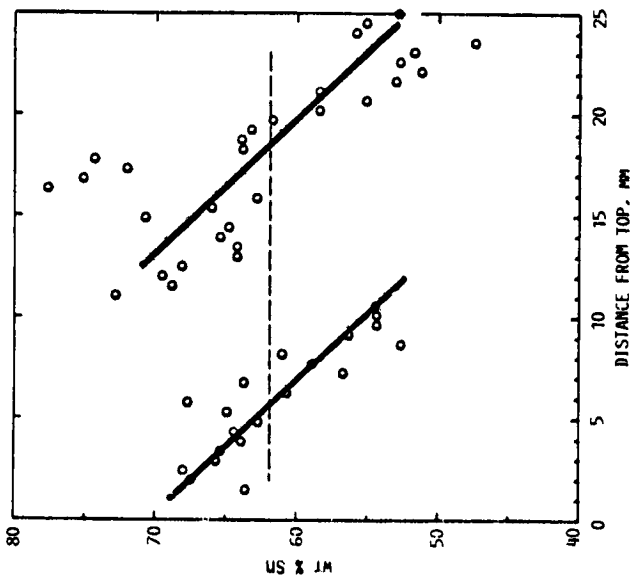
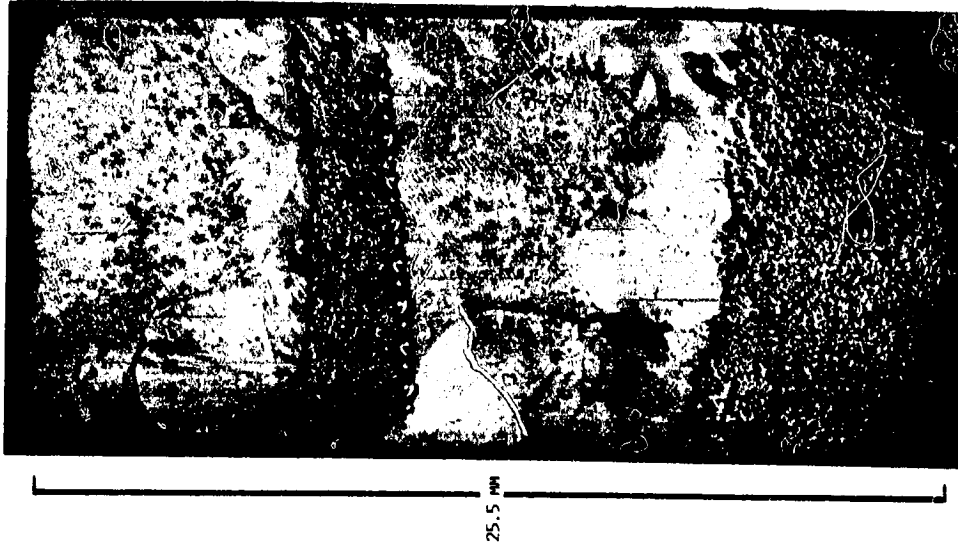
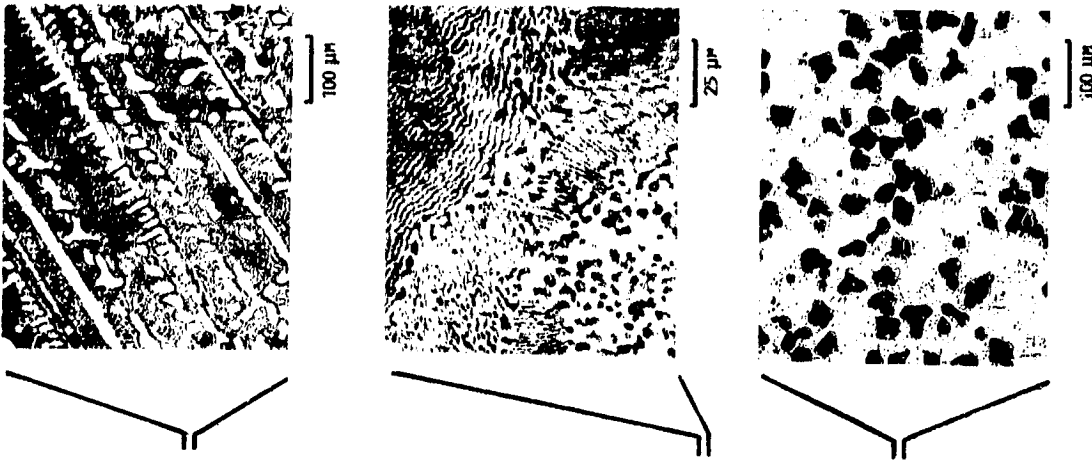


MICROGRAPHS OF LONGITUDINAL CROSS SECTION.
FIGURE 10. - INGOT NUMBER 4, Pb-Sn EUTECTIC INGOT, OIL QUENCHED AND THERMALLY CYCLED, $T_{uc} = 20$ K.



MICROPROBE COMPOSITION MEASUREMENTS WITH BEST FIT
BOLD LINE AND REFERENCE DASH LINE AT 61.9 PERCENT SN.

ORIGINAL PAGE IS
OF POOR QUALITY

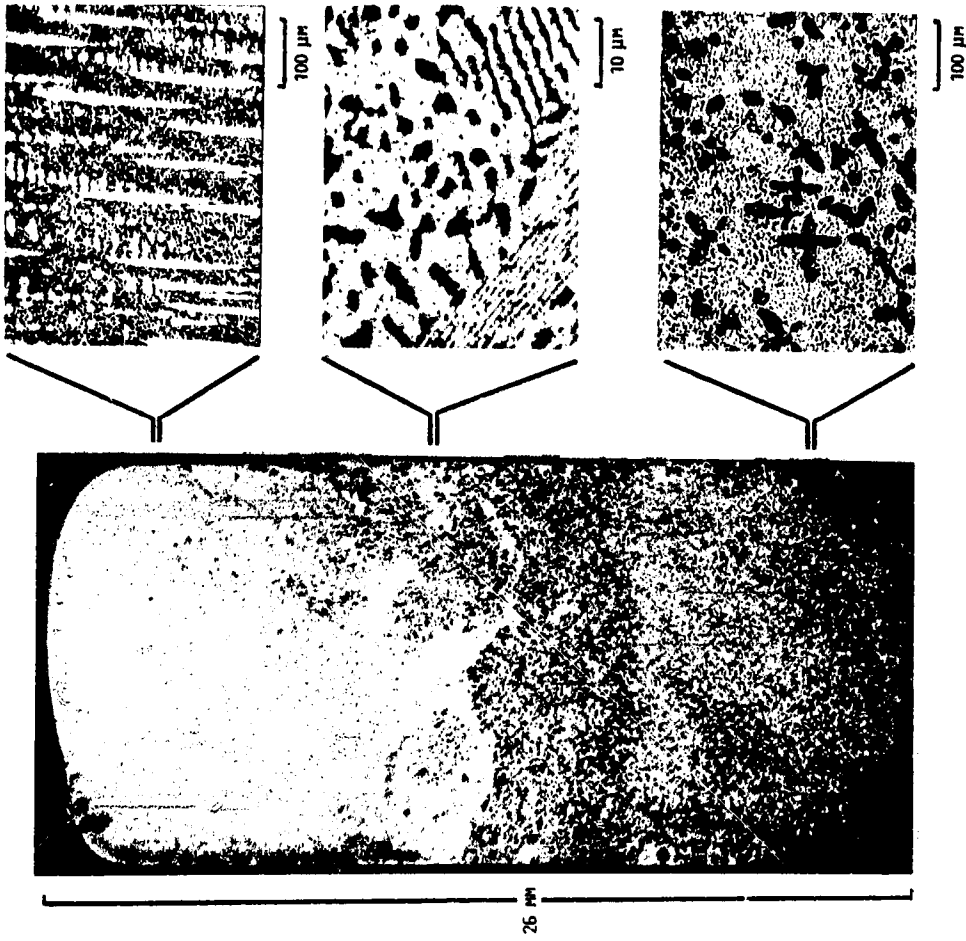


MICROPROBE COMPOSITION MEASUREMENTS.

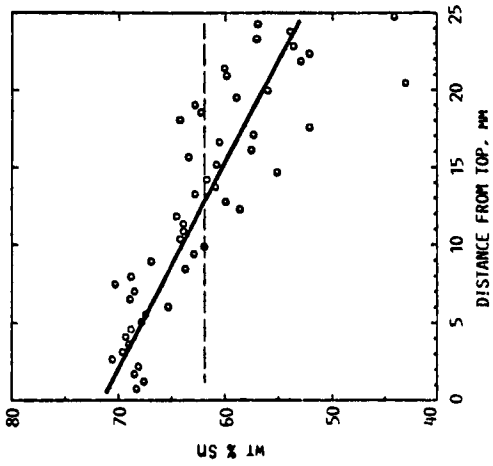
FIGURE 11. - INGOT NUMBER 5, PD-SN EUTECTIC INGOT, SLOW COOLED, THERMALLY CYCLED, AND SOLIDIFIED WITH A STAINLESS STEEL SCREEN NEAR THE CENTER, $T_{DC} = 20$ K.

MICROGRAPHS OF LONGITUDINAL CROSS SECTION.

ORIGINAL PAGE IS
OF POOR QUALITY

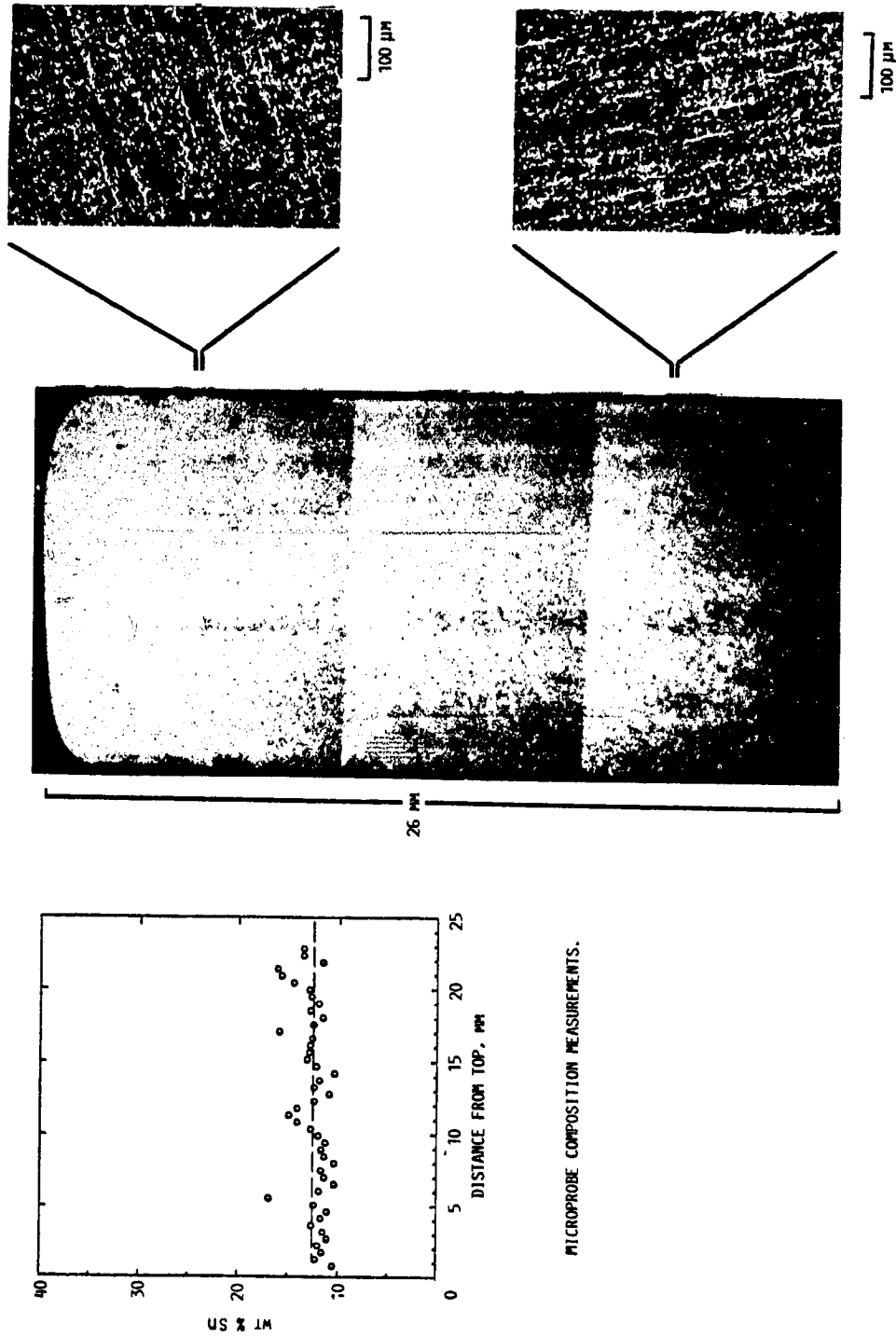


MICROGRAPHS OF LONGITUDINAL CROSS SECTION.
FIGURE 12. - INGOT NUMBER 6, Pd-Sn EUTECTIC INGOT FURNACE QUENCHED IN THE BIF, $T_{UC} = 34$ K.



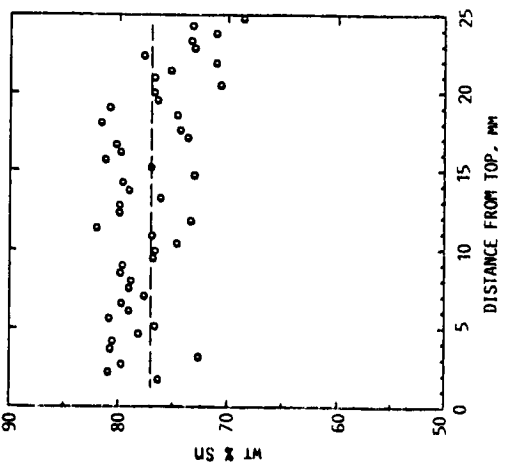
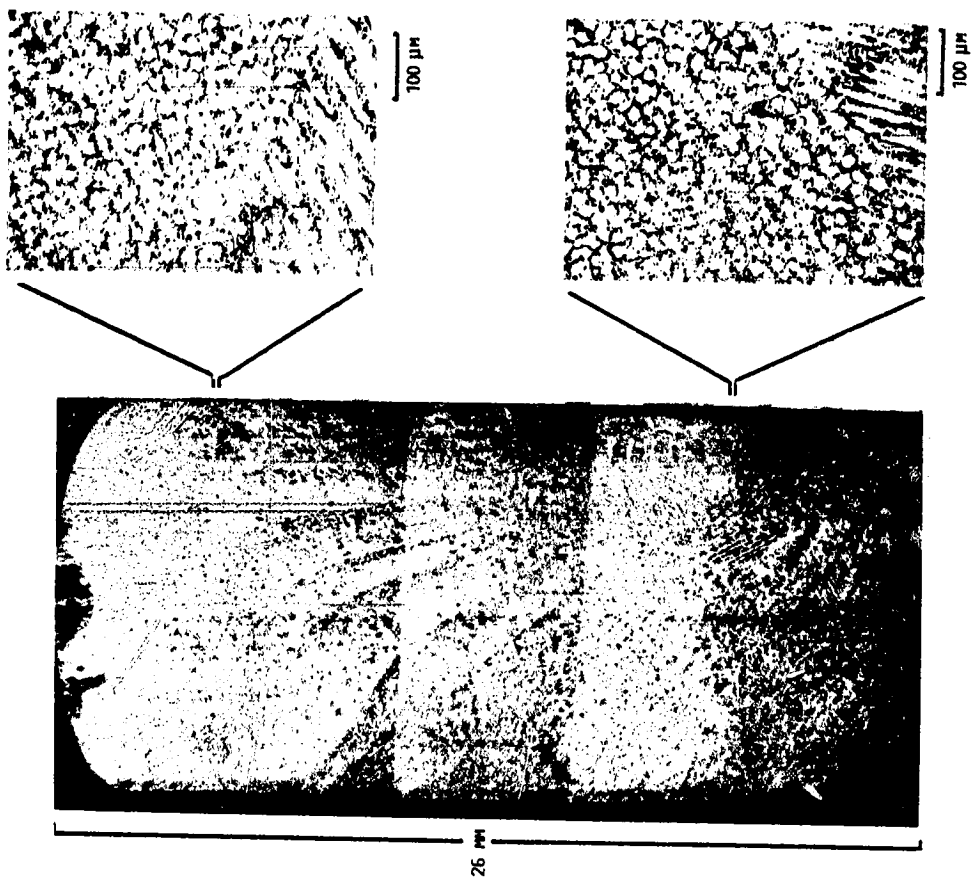
MICROPROBE COMPOSITION MEASUREMENTS WITH
BEST FIT BOLD LINE AND DASHED LINE FOR
REFERENCE AT 61.9 PERCENT Sn.

ORIGINAL PAGE IS
OF POOR QUALITY



MICROGRAPHS OF LONGITUDINAL CROSS SECTION.
FIGURE 13. - INGOT NUMBER, Pb-12.5 wt % Sn INGOT FURNACE QUENCHED IN THE BUF, $T_{uc} = 12$ K.

ORIGINAL PAGE IS
OF POOR QUALITY



MICROPROBE COMPOSITION MEASUREMENTS.

MICROGRAPHS OF LONGITUDINAL CROSS SECTION.

FIGURE 14. - INGOT NUMBER 8, Pd-77 WT % Sn INGOT FURNACE QUENCHED ON THE BUF. $T_{UC} = 31 K.$

ORIGINAL PAGE IS
OF POOR QUALITY

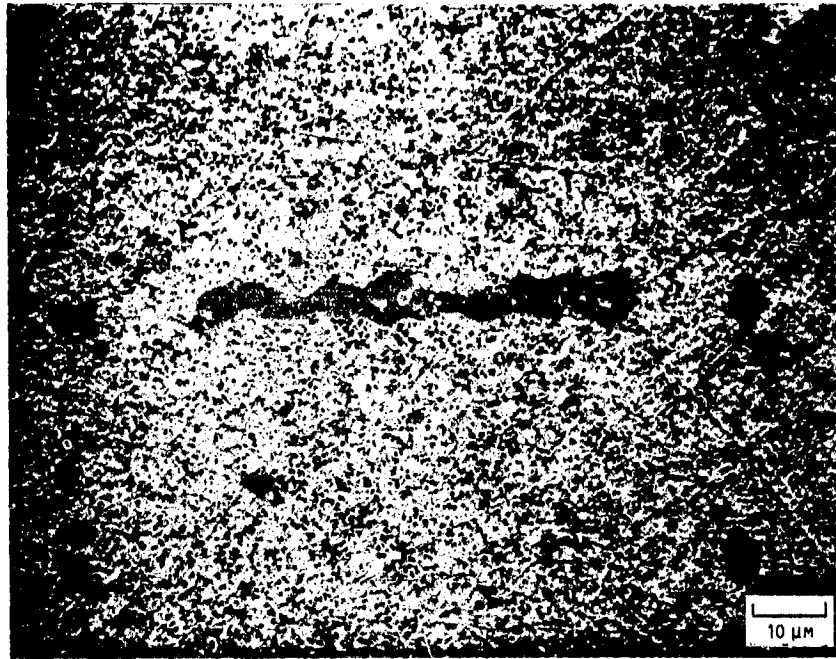


FIGURE 15. - SCANNING ELECTRON MICROSCOPE, BACK SCATTERING MICROGRAPH, DARK LONG AREA IN THE CENTER IS INTERDENDRITIC, EUTECTIC, MICROPROBE COMPOSITIONAL ANALYSIS WAS 89 PERCENT Sn.

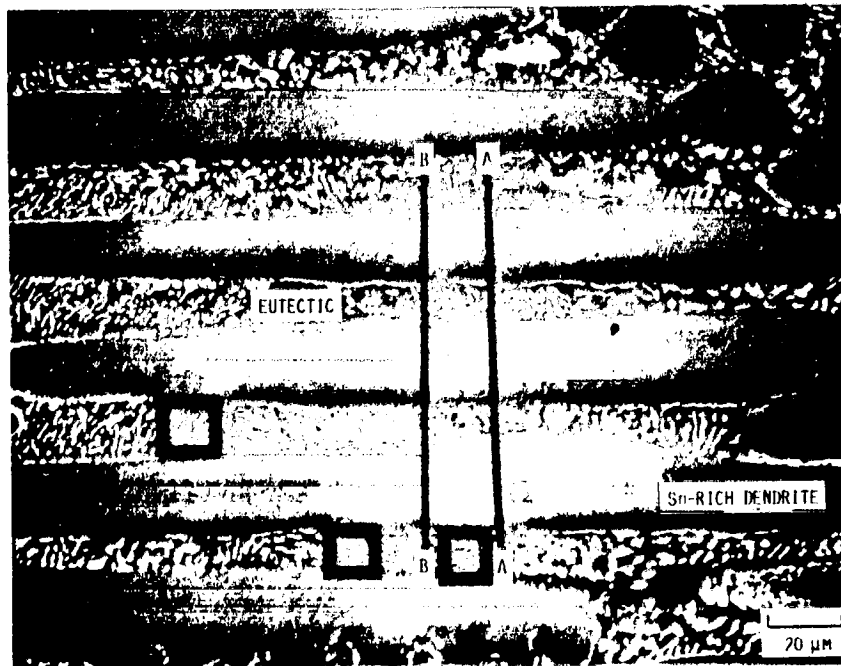
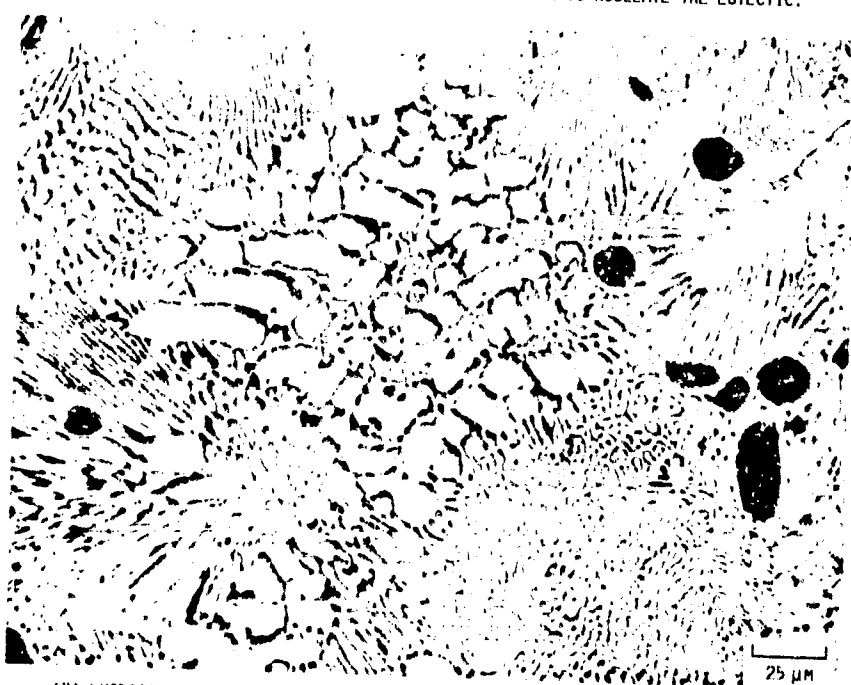


FIGURE 16. - BACK SCATTER SEM MICROGRAPH OF Pb-77 PERCENT Sn INGOT SHOWING SCANS ACROSS THE DENDRITES (AA AND BB) AND EUTECTIC AREAS ANALYZED.

ORIGINAL PAGE IS
OF POOR QUALITY



(A) LEAD-RICH DENDRITES, DARK PHASE, DO NOT APPEAR TO NUCLEATE THE EUTECTIC.



(B) EUTECTIC IS SEEN RADIATING FROM THE Sn-RICH DENDRITES, LIGHT SHADDED PHASE.

FIGURE 17. - OPTICAL PHOTOMICROGRAPHS OF Pb-61.9 PERCENT Sn INGOT UNDERCOOLED 34 K.

Report Documentation Page

1. Report No. NASA TM-102023		2. Government Accession No.		3. Recipient's Catalog No.	
4. Title and Subtitle Macrosegregation and Nucleation in Undercooled Pb-Sn Alloys				5. Report Date May 1989	
				6. Performing Organization Code	
7. Author(s) Henry C. de Groh III				8. Performing Organization Report No. E-4759	
				10. Work Unit No. 674-25-1 5	
9. Performing Organization Name and Address National Aeronautics and Space Administration Lewis Research Center Cleveland, Ohio 44135-3191				11. Contract or Grant No.	
				13. Type of Report and Period Covered Technical Memorandum	
12. Sponsoring Agency Name and Address National Aeronautics and Space Administration Washington, D.C. 20546-0001				14. Sponsoring Agency Code	
15. Supplementary Notes					
16. Abstract <p>A novel technique resulting in large undercoolings in bulk samples (23g) of lead-tin alloys was developed. Samples of Pb-12.5 wt % Sn, Pb-61.9 wt % Sn, and Pb-77 wt % Sn were processed with undercoolings ranging from 4 to 34 K and with cooling rates varying between 0.04 and 4 K/sec. The nucleation behavior of the Pb-Sn system was found to be nonreciprocal. The solid Sn phase effectively nucleated the Pb phase of the eutectic; however, large undercoolings developed in Sn-rich eutectic liquid in the presence of the solid Pb phase. This phenomenon is believed to be mainly the result of differences in interfacial energies between solid Sn-eutectic liquid, and solid Pb-eutectic liquid rather than lattice misfit between Pb and Sn. Large amounts of segregation developed in the highly undercooled eutectic ingots. This macrosegregation was found to increase as undercooling increases. Macro-segregation in these undercooled eutectic alloys was found to be primarily due to a sink/float mechanism and the nucleation behavior of the alloy. Lead-rich dendrites are the primary phase in the undercooled eutectic system. These dendrites grow rapidly into the undercooled bath and soon break apart due to recalescence and Sn enrichment of the liquid. These fragmented Pb dendrites are then free to settle to the bottom portion of the ingot causing the macrosegregation observed in this study. A eutectic Pb-Sn alloy undercooled 20 K and cooled at 4 K/sec had a composition of about Pb-72 wt % Sn at the top and 55% Sn at the bottom.</p>					
17. Key Words (Suggested by Author(s)) Nonreciprocal nucleation; Macrosegregation; Gravity-driven dendrite settling; Eutectic; Lead; Tin; Undercooling				18. Distribution Statement Unclassified - Unlimited Subject Category 26	
19. Security Classif. (of this report) Unclassified		20. Security Classif. (of this page) Unclassified		21. No of pages 34	22. Price* A03